Meta-harzburgites and meta-pyroxenites of the Austroalpine Sieggraben structural complex between Steinbach and Gschorrholz, Austria: An example of subducted mantle

Samila Hrvanović, Marián Putiš & Peter Bačík
Department of Mineralogy and Petrology, Faculty of Natural Sciences, Comenius University, Mlynská dolina, Ilkovičova 6, 842 15 Bratislava, Slovak Republic.
e-mail: hrvanovic@fns.uniba.sk, putis@fns.uniba.sk, bacikp@fns.uniba.sk

AGEOS

Metaharzburgity a metapyroxenity sieggrabenského štruktúrneho komplexu austroalpinika medzi Steinbachom a Gschorrholzom, Rakúsko: príklad subdukovaného plášťa

Abstract: The Sieggraben structural complex occupies a middle position in the Austroalpine basement nappe system in the Eastern Alps. Investigated area is located at the southeastern part of Austria between the Steinbach and Gschorrholz villages (approximately 150 km south of Vienna). The aim of this paper is to characterize petrographic and mineral chemical composition of meta-harzburgites and meta-pyroxenites. Identified mineral assemblage from selected microstructures of massive to sheared meta-pyroxenite and meta-harzburgite is composed of Ol, Opx, Cpx, zoned Amp, Chl, serpentine group minerals Atg/Ctl, spinel group minerals Spl, Hc and rare Tlc. Meta-harzburgites and meta-pyroxenites are members of a subduction complex.

Key words: Eastern Alps, Sieggraben structural complex, meta-harzburgite, meta-pyroxenite, petrography, mineral chemistry

1. INTRODUCTION

The Sieggraben eclogite-bearing structural basement complex at the south-eastern margin of the Eastern Alps contains metaultramafics (e.g., Putiš et al. 2000, 2002). According to Tollmann (1980), the Sieggraben structural complex is a part of the Middle Austroalpine tectonic unit in the Eastern Alps (Fig. 1). Although this complex is most likely a remnant of a pre-Alpine basement, it has a strong Alpine polyphase metamorphic-deformational overprint (Putiš et al. 2000, 2002). The geological and geotectonic evolution of this complex was characterized by Tollmann (1980), Frank et al. (1987), Frisch and Neubauer (1989), Neubauer et al. (1992), Neubauer and Frisch (1993), Neubauer (1994) and Froitzheim et al. (1996). The results of isotopic mineral and whole-rock dating were published by Dallmeyer et al. (1996, 1998), Thöni and Jagoutz (1993), Thöni (1999), Thöni et al. (2008) and Putiš et al. (1994, 2000) reporting Alpine metamorphic overprint ages. Based on the petrological and geothermobarometric data, the evolutionary P–T pathway of the host eclogite-bearing complex was suggested by Putiš et al. (2002) and Kromel et al. (2011).

Data on geological mapping, petrotectonics and petrology were published by Putiš et al. (1994, 2000, 2002) and Korikovsky et al. (1998). A brief characterization of petrography and mineral chemistry of the Sieggraben meta-harzburgites was reported by Hrvanović et al. (2014) from the area of Sieggraben and Schwarzenbach.

The goal of this paper is to present petrographic and mineral chemistry data related to evolutionary stages of a host meta-harzburgite and crosscutting meta-pyroxenite dikes from the Sieggraben structural complex in the area between the Steinbach and Gschorrholz villages in southeastern Austria (Fig. 1a). The studied mineral assemblages of meta-harzburgites and meta-pyroxenites provide rare information on tectonometamorphic evolution of mantle fragments in a subduction zone.

Mineral abbreviations used in our text, tables and figures are after Whitney and Evans (2010): Amp = amphibole, Atg = antigorite, Bt = biotite, Cal = calcite, Chl = chlorite, Chr = chromite, Clc = clinochlore, Ctl = chrysotile, Cpx = clinopyroxene, Di = diopside, En = enstatite, Fs = ferrosilite, Fo = forsterite, Grt = garnet, Hc = hercynite, Jd = jadeite, Mag = magnetite, Mhb = magnesiohornblende, Ms = muscovite, Ol = olivine, Omp = omphacite, Opx = orthopyroxene, Pl = plagioclase, Ph = phengite, Prg = pargasite, Qz = quartz, Rt = rutile, Srp = serpentine group, Spl = spinel, Tlc = talc, Tr = tremolite, Ts = tschermakite, Wo = wollastonite, Zo = zoisite, besides Carb = carbonates.

2. GEOLOGICAL SETTING OF THE SIEGGRABEN STRUCTURAL COMPLEX

The tectonostratigraphy of the Austroalpine (AA) structural complexes is based on the work of Tollmann (1980). Schmid et al. (2004) avoided Middle AA terminology, considering this part of the AA Unit as belonging to the Upper Austroalpine Unit after the Cretaceous collision (Neubauer 1994).

Manuscript received 3 March 2015
Revised version accepted 28 May 2015

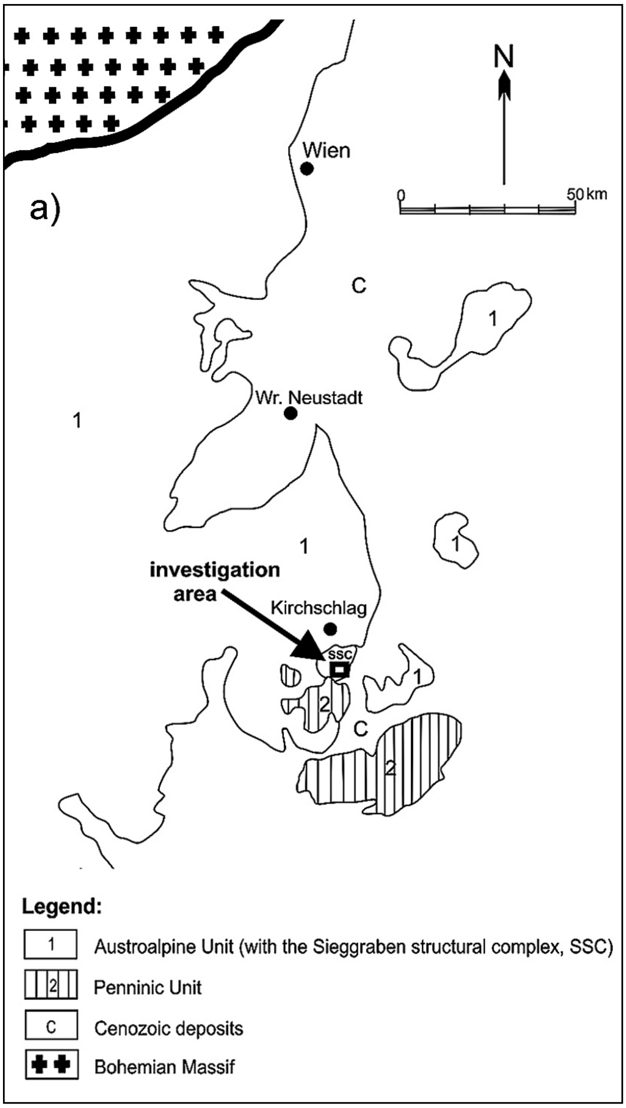

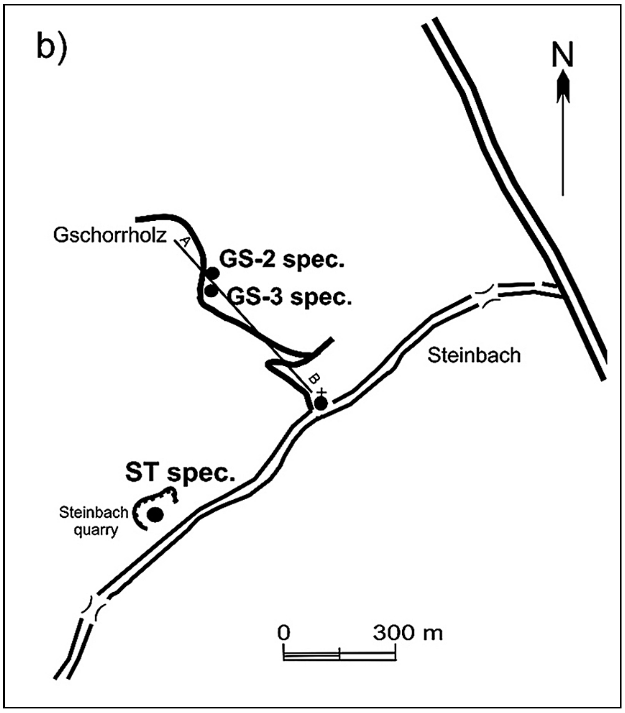

Fig. 1. a) Tectonic sketch of basic tectonic units of the Eastern Alps (source: http://www.zonu.com/detail-en/2011-06-29-13972/Geological-map-of-Austria.html). **b)** Topographic sketch (source: http://www.austrianmap.at) of the investigated area with studied specimens location and a cross-section line A-B (see 1c). **c)** Geological cross-section of the MAA structural complex.
Obr. 1. a) Tektonická skica hlavných tektonických jednotiek Východných Álp (zdroj: http://www.zonu.com/detail-en/2011-06-29-13972/Geological-map-of-Austria.html). **b)** Topografická skica (zdroj: http://www.austrianmap.at) skúmanej oblasti s lokalizáciou študovaných vzoriek a líniou geologického rezu A-B (pozri 1c). **c)** Geologický rez štruktúrneho komplexu stredného austroalpinika.

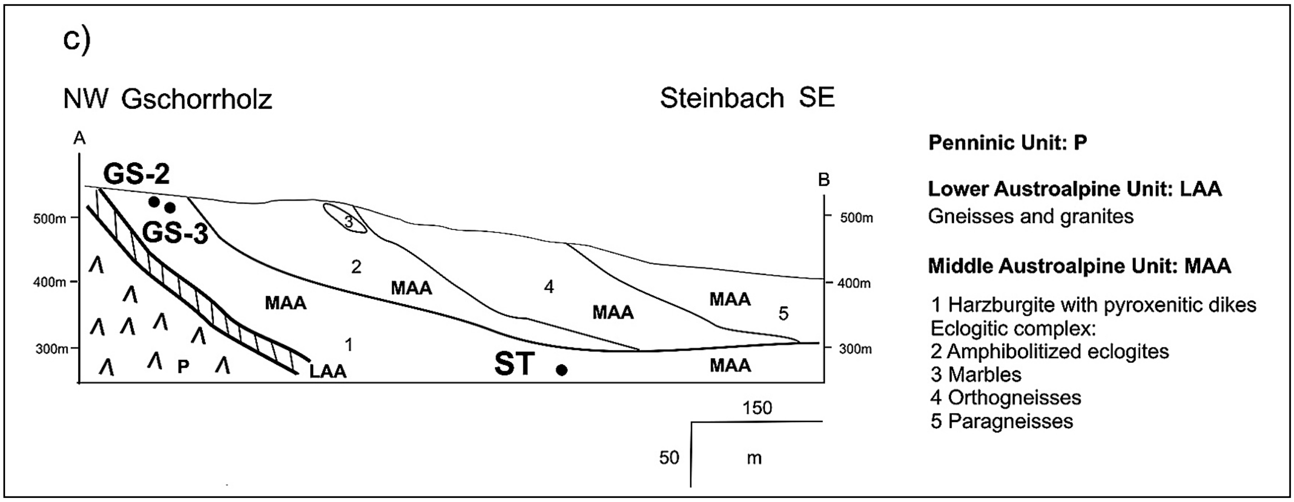

Field geological-structural mapping of the Sieggraben structural complex (SSC) in the area around Sieggraben (Putiš et al. 2000, 2002) determined two main types of thrust-faults and related meso- and microstructures: Early Cretaceous higher-temperature structures are defined by NNW–SSE trending high-pressure D1 mineral lineations reflected in high-pressure phases of Cpx–Omp, Zo and Amp–Prg, and also in the mostly medium-temperature D2 lineations of Qz, Pl, Amp in ductile layered mylonites. These higher-temperature structures are recognizable only in the internal parts of the AA SSC, and they are overprinted by D3 lower temperature WSW dipping stretching lineations in ductile blastomylonitic microstructures; particularly evident in the hanging wall. Low-angle normal faults, most likely active during late Cretaceous to Early Neogene, were observed in the footwall LAA Grobgneis and Wechsel structural complexes. The top-to-WSW movement along the low-temperature lineation is defined by newly formed fine-grained white mica aggregates (Ms, Ph), Bt and Chl in combination with asymmetric S–C type microstructures of metapelites and granitic orthogneisses.

The pre-Alpine (Variscan) metamorphic event is supposed in the SSC. This is inferred from the U/Pb upper intercept age of zircon, apatite and monazite at 312.7±7.9 Ma, and/or the whole-rock Rb/Sr isotope age of 289±16 Ma, dating the granitic protoliths of the Sieggraben orthogneisses (Putiš et al. 2000). These dates indicate the magmatic age of a granitic precursor which intruded a metamorphosed Early Paleozoic crustal complex. However, the lower intercept age of 103±14 Ma recorded in Putiš et al. (1994, 2000) clearly indicates the age of the main Alpine (Early Cretaceous) higher-temperature (and higher pressure) metamorphic overprint. The U/Pb lower discordia intercept age of granitic orthogneisses zircon, apatite and monazite is interpreted as cooling of the SSC during exhumation along a deep crustal extension normal detachment fault between 750–500°C (Putiš et al. 2000).

The Sieggraben structural complex (Kümel 1935; Tollmann 1977) is composed of metapelites (gneisses, micaschists), metabasites (eclogites, amphibolites, metagabbros), metaultramafics (serpentinites), metagranitoids (leucocrate metagranites, metapegmatites), impure metacarbonates and calc-silicate rocks (impure marbles). The rocks of the SSC indicate two higher-temperature and high-to-medium pressure metamorphic stages reported as D1 and D2 deformation stages. D1 denotes burial in a subduction-related wedge and subduction channel, while D2 is a later unroofing and exhumation phase (Putiš et al. 2000, 2002; Kromel et al. 2011). The D1 prograde burial stage resulted in Omp formation with almost 40 % Jd, Prg-Amp1, Zo, Grt and Rt in eclogites, the D2 exhumation stage is, in contrast, reflected by Cpx2–Pl symplectites after Omp, and Ts-Amp2 coronas (± Pl, Bt) around Grt (Putiš et al., 2000, 2002).

The D1 temperature had previously been estimated at 610–650°C at minimum pressure of 16–17 kbar, and D2 at 700°C and 12 kbar (Kromel et al., 2011). Compared to model of Putiš et al. (2002), this eclogite-facies metamorphic temperature was estimated slightly lower at higher minimum pressure. Petrography and mineral chemistry of the Sieggraben meta-harzburgites was reported by Hrvanović et al. (2014).

The SSC between Steinbach and Gschorrholz (Fig. 1b) is built of mafic eclogites strongly retrogressed to amphibolites, para- and orthogneisses, with thin marble layers. This part of the SSC does not contain any layer or even tectonic lens of meta-ultramafics, the latter exposed separately in large km-size block(s) in direct tectonic contact with the SSC (Fig. 1c). The host meta-harzburgites occur below the described eclogitic complex; their contact is tectonic (sheared) and strongly weathered. The harzburgite is crosscut by at least two systems of pyroxenite dikes. Our study was focused on mineral assemblages of the host meta-harzburgite and the crosscutting meta-pyroxenitic dikes as well.

3. MATERIALS AND METHODS

Hand specimens were collected from a road cut between the Gschorrholz and Steinbach (Fig. 1b) villages (all GS-2 specimens: N 47° 28.665', E 16°18.571'; all GS-3 specimens: N 47° 28.667', E 16°18.552'), and a quarry in Steinbach (all ST specimens: N 47° 28.273', E 16°18.436'). Mineral composition and microstructures were investigated in 13 selected polished sections by polarized-light microscope Leica DM2500P at the Department of Mineralogy and Petrology, Comenius University in Bratislava. Chemical compositions of minerals were determined by a Cameca SX-100 electron microprobe at the State Geological Institute of Dionýz Štúr in Bratislava. Analytical conditions were at 15 kV accelerating voltage and 20 nA beam current. Cameca Peak Sight v 4.2 software was used for data recalculation. We used following standards for calibration of the given elements (in brackets): albite (Na *Kα*), wollastonite (Si *Kα*, Ca *Kα*), orthoclase (K *Kα*), forsterite (Mg *Kα*), Al_2O_3 (Al *Kα*), fayalite (Fe *Kα*), rhodonite (Mn *Kα*), metallic Cr (Cr *Kα*), V (V *Kα*), Ni (Ni *Kα*), TiO_2 (Ti *Kα*). The beam diameter used was 5 and 10 μm, and/or 1-3 μm for exsolution lamellae and symplectites.

Mineral formulae were calculated on the basis of 4 oxygen anions for olivine, 15 (eNK) cations for amphibole, 4 cations for pyroxene, 3 cations for spinel, 14 oxygen anions for the minerals of serpentine group and chlorite. Fe^{3+} was calculated from charge balance.

4. RESULTS

Investigated metaultramafic rocks from Steinbach and Gschorrholz are meta-harzburgites and meta-pyroxenites. Meta-harzburgites are composed of Ol, Opx, Cpx, Amp, spinel group minerals, serpentine group minerals Chl and rare Carb. Meta-pyroxenites are composed of Opx, Cpx, Ol, Amp, spinel group minerals, serpentine group minerals, Chl and rare Tlc.

Macroscopically meta-harzburgites are dark-green, more or less sheared rocks with fine-grained serpentinized groundmass and visible pale elongated Opx, less Cpx porphyroblasts with size of 0.3 to 0.6 mm across (Fig. 2a). Meta-pyroxenites are pale greenish rocks which occur as dikes in meta-harzburgite. There are two macroscopic varieties of meta-pyroxenites: 1) coarse grained rocks with compact aggregates of pyroxenes (Fig. 2b); 2) sheared rocks with elongated porphyroblasts of pyroxenes in fine grained metamorphic matrix with amphiboles.

4.1. Petrography and mineral chemistry of meta-harzburgite

Olivine has anhedral grains, clear relief with characteristic high interference colour in typical mesh structure of serpentine minerals (Fig. 3a, b). It occurs in metamorphic matrix and as inclusion

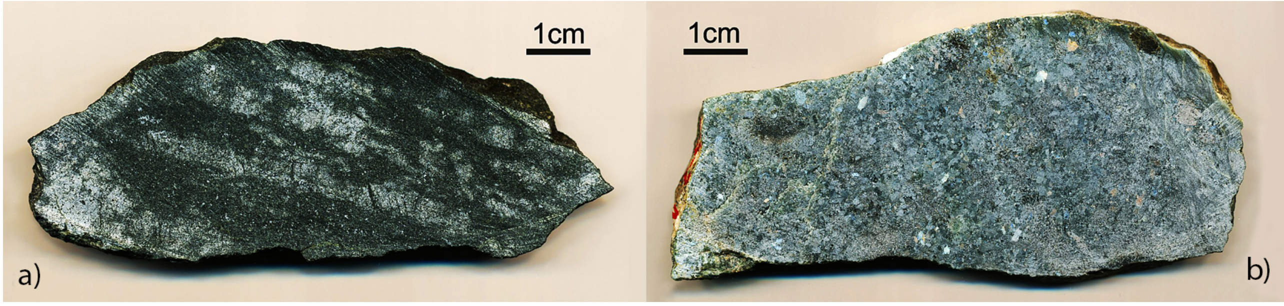

Fig. 2. Cut surfaces of **a)** meta-harzburgite from Steinbach (sample ST-3), **b)** meta-pyroxenite from Gschorrholz area (sample GS-2-1).

Obr. 2. Prierez a) vzorky meta-harzburgitu zo Steinbachu (vzorka ST-3), b) vzorky meta-pyroxenitu z Gschorrholzu (vzorka GS-2-1).

Tab. 1. Representative mineral analyses of Ol, Opx, Cpx and Spl in meta-harzburgite.

Tab. 1. Reprezentačné analýzy Ol, Opx, Cpx a Spl v meta-harzburgite.

Sample	ST-5	ST-S1	ST-3	ST-5	ST-5	ST-5	ST-S1	ST-S1	ST-5
Mineral	Ol	Ol	Opx	Opx	Cpx	Cpx	Spl	Hc	Hc
Analyses No.	An 1	An 31	An 1	An 32	An 14	An 3	An 19	An 8	An 26
wt %									
SiO_2	41.53	41.07	56.78	57.12	55.34	54.58	0.04	0.02	0.00
TiO_2	0.00	0.00	0.02	0.04	0.03	0.01	0.13	0.15	0.22
Al_2O_3	0.04	0.00	0.92	1.35	0.65	0.74	26.93	29.79	23.02
V_2O_3	0.00	0.00	0.00	0.00	0.00	0.00	0.25	0.21	0.32
FeO	9.14	9.64	6.19	6.29	1.63	1.78	31.27	31.35	37.81
MnO	0.10	0.17	0.17	0.17	0.04	0.05	0.40	0.44	0.49
MgO	49.27	49.07	36.01	35.21	17.68	17.38	11.26	9.50	7.02
CaO	0.00	0.04	0.12	0.16	25.13	25.32	0.01	0.00	0.03
Na_2O	0.03	0.01	0.00	0.00	0.16	0.18	0.00	0.00	0.00
K_2O	0.02	0.00	0.00	0.00	0.00	0.01	0.00	0.00	0.00
Cr_2O_3	0.00	0.00	0.20	0.20	0.19	0.23	28.03	27.58	29.38
NiO	0.46	0.36	0.08	0.03	0.05	0.03	0.29	0.21	0.19
Total	100.58	100.37	100.50	100.57	100.90	100.32	98.61	99.24	98.49
a.p.f.u.									
Si^{4+}	1.012	1.004	1.938	1.953	1.989	1.975	0.000	0.000	0.000
Ti^{4+}	0.000	0.000	0.000	0.000	0.001	0.000	0.003	0.003	0.005
Al^{3+}	0.001	0.000	0.037	0.055	0.028	0.031	0.977	1.075	0.873
Cr^{3+}	0.000	0.000	0.000	0.005	0.005	0.007	0.682	0.668	0.747
Fe^{3+}	0.000	0.000	0.055	0.032	0.000	0.025	0.338	0.253	0.374
Fe^{2+}	0.186	0.197	0.122	0.148	0.052	0.029	0.467	0.550	0.643
Mg^{2+}	1.790	1.788	1.833	1.795	0.947	0.937	0.517	0.434	0.337
Mn^{2+}	0.002	0.004	0.005	0.005	0.001	0.002	0.010	0.011	0.013
Ca^{2+}	0.000	0.001	0.004	0.006	0.968	0.981	0.000	0.000	0.001
Ni^{2+}	0.009	0.007	0.000	0.000	0.000	0.000	0.006	0.005	0.005
Na^{+}	0.000	0.000	0.000	0.000	0.011	0.013	0.000	0.000	0.000
Total	3.000	3.000	3.994	3.999	4.000	3.999	3.000	2.999	3.000
Fo	90.578	90.078							
Wo					48.921	49.383			
En					48.429	49.107			
Fs					2.649	1.510			
2Ti/(2Ti+Al+Cr)							0.004	0.004	0.006
$2Fe^{3+}/(2Fe^{3+}+Al+Cr)$							0.289	0.225	0.316
$Fe^{2+}/(Fe^{2+}+Mg)$							0.475	0.559	0.656
Cr/(Cr+Al)							0.411	0.383	0.461

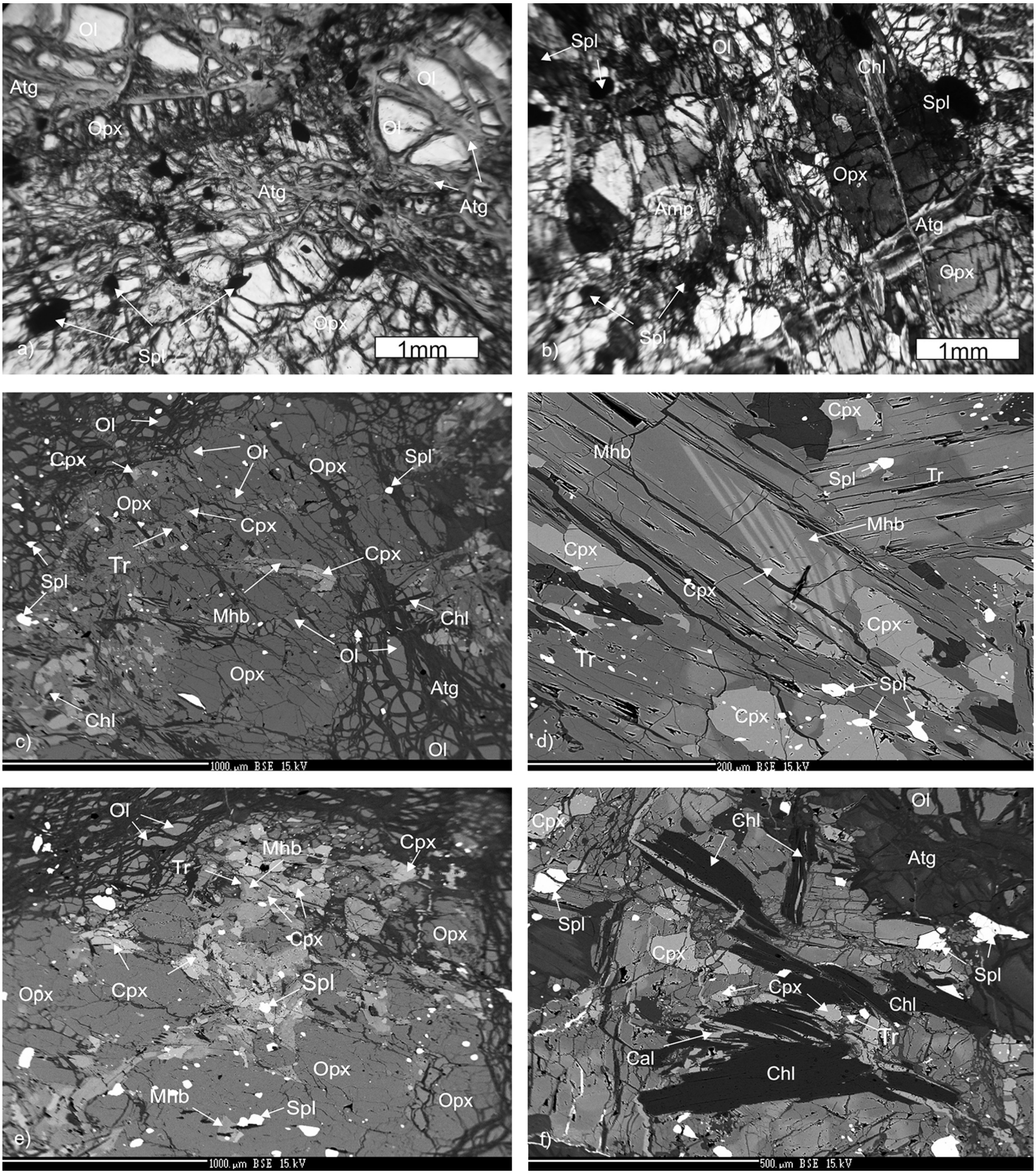

Fig. 3. Photomicrographs **a–b)** and back-scattered electron (BSE) images **c–f)** of meta-harzburgite. **a)** Plain-polarized light microscopic image of Opx and Ol porphyroblasts with mesh structure in the metamorphic matrix serpentine group minerals (sample ST-S1). **b)** Crossed-polarized light microscopic image of metamorphic Opx, Ol, Spl, Amp, Chl, Atg/Ctl (sample ST-3). **c)** Granoblastic matrix of Ol, Opx, Cpx and Spl with ingrowing Chl and Atg/Ctl (sample ST-5). **d)** Exsolution lamellae of low-Al Cpx in the middle part of Mhb grain (sample ST-5). **e)** Opx porphyroblasts ingrown and overgrown by Cpx and Mhb granoblastic aggregate (sample ST-S1). **f)** Hydrated and carbonatized domains rich in Tr, Chl and Atg/Ctl (sample ST-S2).

Obr. 3. Fotografie mikroštruktúr meta-harzburgitu a–b) zobrazených aj v spätne rozptýlených elektrónoch c–f). a) Fotografia porfyroblastov Opx a Ol v štruktúre metamorfného matrixu minerálov serpentínovej skupiny (vzorka ST-S1) v polarizovanom svetle pri rovnobežných nikoloch. b) Fotografia metamorfného Opx, Ol, Spl, Amp, Chl, Atg/Ctl (vzorka ST-3) v polarizovanom svetle pri skrížených nikoloch. c) Matrix granoblastického Ol, Opx, Cpx and Spl s prerastajúcim Chl a Atg/Ctl (vzorka ST-5). d) Exsolučné lamely nízkohlinitého Cpx v strednej časti blastov Mhb (vzorka ST-5). e) Porfyroblasty Opx prerastené granoblastickým agregátom Cpx and Mhb (vzorka ST-S1). f) Hydratované a karbonizované mikrooblasti s prevahou Tr, Chl a Atg/Ctl (vzorka ST-S2).

in Opx (Fig. 3c). Grains of Ol have no chemical zoning; they have typical metamorphic composition with 89.14 to 91.62 mol. % Fo found from 19 analyses (Tab. 1).

Orthopyroxene has high relief and no pleochroism. Porphyroblasts are surrounded by metamorphic Ol-rich matrix (Fig. 3a-c). It is low-Al metamorphic Opx with Al_2O_3 0.5 to 1.8 wt. % (found from 17 analyses), partly altered into Atg, Chl and Ctl along irregular cracks. The Opx has composition of enstatite with Mg from 1.76 to 1.88 *apfu* found from 17 analyses (Fig. 5a; Tab. 1). Orthopyroxene also occurs as granoblastic grains in the metamorphic matrix. Chemical composition of Opx porphyroblasts and granoblastic Opx from metamorphic matrix is very similar.

Clinopyroxene occurs as anhedral grains in aggregates in metamorphic matrix (Fig. 3c,d). Exsolution lamellae of low-Al Cpx are observable in Amp (Fig. 3d). Some anhedral grains of Cpx often ingrows Ol aggregates, or intergrows with Opx (Fig. 3e). Clinopyroxene has diopside composition with Ca 0.96 to 0.99 Clinopyroxene has diopside composition with Ca 0.96 to 0.99 *apfu* found from 32 analyses (Fig. 5a; Tab. 1). The chemical composition of anhedral grains and exsolution lamellae is the similar; both are low-Al Cpx.

Amphibole is porphyroblastic or granoblastic and occurs in metamorphic matrix. Grains show zonal chemical composition. The central part of Amp is composed of zonal magnesiohornblende which is rimmed by Tr (Figs 3d, 5b). This central part of Amp shows gradually increasing content of Al, Na, K and Ti from the center to the rim of grain (Tab. 2). The central part of lower-Al magnesio-hornblende often shows Cpx exsolution lamellae and it is rimmed by magnesio-hornblende (richer in Na and Al) to pargasite, without Cpx lamellae (Fig. 3d). Tremolite ingrows and replaces Opx, Cpx and occurs also as individual grains in the metamorphic matrix with Cpx (Fig. 3c–e).

Spinel group minerals are represented by anhedral grains in size of 0.1 to 0.2 mm uniformly distributed in the metamorphic matrix, or as inclusions in Opx (Fig. 3a–d). There are more chemical varieties of the spinel group minerals: spinel, hercynite, with Cr content from 0.67 to 0.79 *apfu* found from 5 analyses (Fig. 5c; Tab. 1). Magnetite is often present too, but we do not deal with this mineral in detail in this work.

Chlorite grains are flaky, randomly oriented, with different size, produced by alteration of Ol or Opx (Fig. 3b,c,f). According to calculated structural formula it is clinochlore containing ca. 4.5 Mg *apfu* (Fig. 5d; Tab. 3).

Serpentine group minerals form mesh structure of Atg and Ctl after Ol, or together with Amp replace Opx along cracks (Figs 3a–c,f, 5e; Tab. 3). Iron content in Atg is consistent with Fe content in Ol and/or Opx which are partly replaced with this Atg. Relatively younger Ctl occurs in aggregates with Atg and Mg-Chl.

Tab. 2 Representative chemical composition of Amp in meta-harzburgite.
Tab. 2 Reprezentačné analýzy Amp v meta-harzburgite.

Sample	ST-5	ST-5	ST-5	ST-5	ST-5	ST-S1
Mineral	Mhb	Mhb	Mhb	Mhb	Tr	Tr
Analyses No.	An 37	An 47	An 9	An 12	An 8	An 1
wt %						
SiO_2	51.68	51.07	50.09	46.91	57.57	56.13
TiO_2	0.10	0.07	0.15	0.17	0.03	0.05
Al_2O_3	6.63	6.74	9.55	11.67	1.86	2.66
Cr_2O_3	0.46	0.52	0.46	0.90	0.11	0.09
FeO	3.27	3.20	4.01	4.61	2.13	2.40
MnO	0.05	0.05	0.04	0.05	0.04	0.10
MgO	21.12	20.90	19.70	18.12	22.63	22.70
NiO	0.15	0.13	0.09	0.13	0.12	0.08
CaO	13.17	13.24	12.96	12.91	13.52	13.65
Na_2O	0.92	1.02	1.27	1.34	0.11	0.24
K_2O	0.08	0.08	0.16	0.68	0.01	0.06
Cl	0.00	0.01	0.01	0.00	0.00	0.02
Total	97.63	97.03	98.49	97.50	98.14	98.17
a.p.f.u.						
Si^{4+}	7.150	7.116	6.923	6.615	7.849	7.655
Al^{3+}T	0.850	0.884	1.077	1.385	0.151	0.345
T-sum.	8.000	8.000	8.000	8.000	8.000	8.000
Ti^{4+}	0.010	0.008	0.015	0.018	0.003	0.005
Al^{3+}Z	0.231	0.223	0.479	0.555	0.149	0.083
Cr^{3+}	0.050	0.057	0.050	0.100	0.012	0.010
V^{3+}	0.000	0.000	0.000	0.000	0.000	0.000
Mg^{2+}	4.356	4.341	4.058	3.810	4.599	4.615
Mn^{2+}	0.005	0.005	0.005	0.007	0.005	0.011
Fe^{3+}	0.287	0.301	0.148	0.203	0.000	0.168
Fe^{2+}	0.092	0.073	0.315	0.341	0.243	0.105
Zn^{2+}	0.000	0.000	0.000	0.000	0.000	0.000
Ni^{2+}	0.017	0.016	0.010	0.015	0.014	0.009
C-sum.	5.048	5.023	5.080	5.050	5.025	5.006
Ca^{2+}	1.952	1.977	1.920	1.950	1.975	1.994
Na^{+}	0.048	0.023	0.080	0.050	0.025	0.006
B–sum.	2.000	2.000	2.000	2.000	2.000	2.000
Na^{+}	0.198	0.252	0.261	0.318	0.003	0.058
K^{+}	0.015	0.013	0.028	0.122	0.001	0.010
A–sum.	0.213	0.265	0.289	0.440	0.004	0.068
Cl^{-}	0.000	0.002	0.003	0.000	0.000	0.005
OH^{-}	2.000	1.998	1.997	2.000	2.000	1.995

4.2. Petrography and mineral chemistry of meta-pyroxenite

Olivine occurs as anhedral grains in size 20 μm in the metamorphic matrix characterized by typical metamorphic composition. It has 90.43 to 92.13 mol. % of Fo component found from 14 analyses (Tab. 4). Some of grains are altered in talc and some occur in symplectite with Spl.

Orthopyroxene occurs as anhedral porphyroblasts in the fine grained metamorphic matrix of low-Al Cpx, low-Al Opx and Amp (Fig. 4a,b; Tab. 4). Orthopyroxene porphyroblasts are locally broken down to Opx-Cpx symplectites, partly replaced

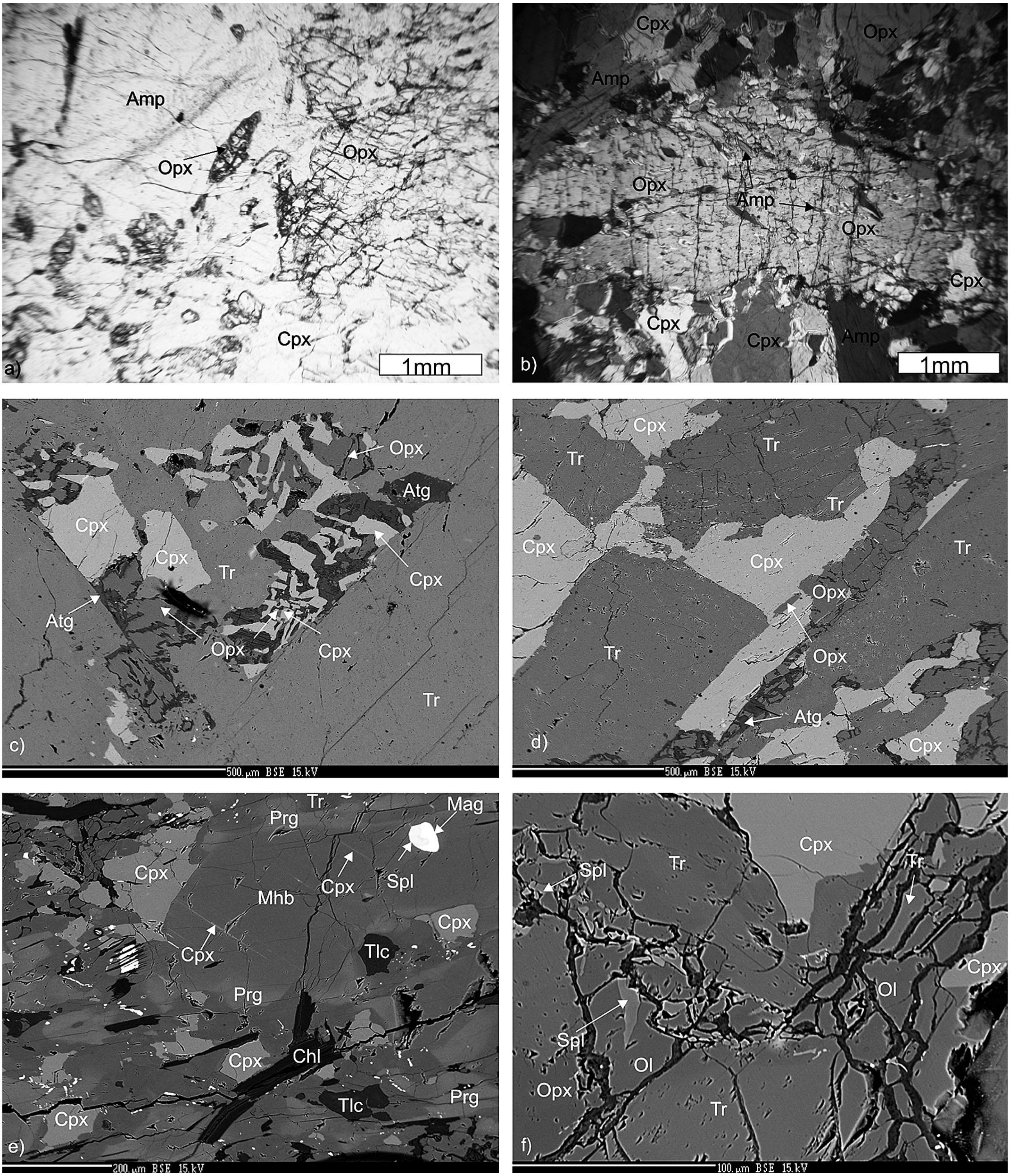

Fig. 4. Photomicrograph **a–b)** and **c–f)** BSE of meta-pyroxenite. **a)** Plain-polarized light microscopic image of Opx and Amp porphyroblasts (sample GS-2c). **b)** Crossed-polarized light microscopic image of Opx porphyroblast in the metamorphic matrix of Opx, Cpx and Amp (sample GS-2-2). **c)** Prograde-metamorphic Opx-Cpx symplectite in Opx porphyroblast (sample GS-2a). **d)** Amphibolization (Tr) of Opx-Cpx matrix (sample GS-Px1). **e)** Cpx, Opx and Mhb porphyroblasts, rimmed by Tr. Central part of Mhb with Cpx exsolution lamellae, and Prg rim (sample GS-3-1). **f)** Ol-Spl symplectite in matrix of Opx, Cpx and Ol. Tr as a retrograde phase (sample GS-2c).

Obr. 4. Fotografie mikroštruktúr meta-pyroxenitu a–b) zobrazených aj v spätne rozptýlených elektrónoch c–f). a) Fotografia porfyroblastov Opx a Amp (vzorka GS-2c) v polarizovanom svetle pri rovnobežných nikoloch. b) Fotografia porfyroblastov Opx v metamorfnom matrixe Opx, Cpx a Amp (vzorka GS-2-2) v polarizovanom svetle pri skrížených nikoloch. c) Prográdno-metamorfný Opx-Cpx symplektit v porfyroblaste Opx (vzorka GS-2a). d) Amfibolizácia (Tr) Opx-Cpx matrixu (vzorka GS-Px1). e) Porfyroblasty Cpx, Opx a Mhb lemované Tr. Centrálna časť Mhb má exsolučné lamely Cpx a je lemovaná Prg (vzorka GS-3-1). f) Ol-Spl symplektit v matrixe Opx, Cpx a Ol. Tr ako retrográdna fáza (vzorka GS-2c).

ACTA GEOLOGICA SLOVACA, 7(1), 2015, 73–84

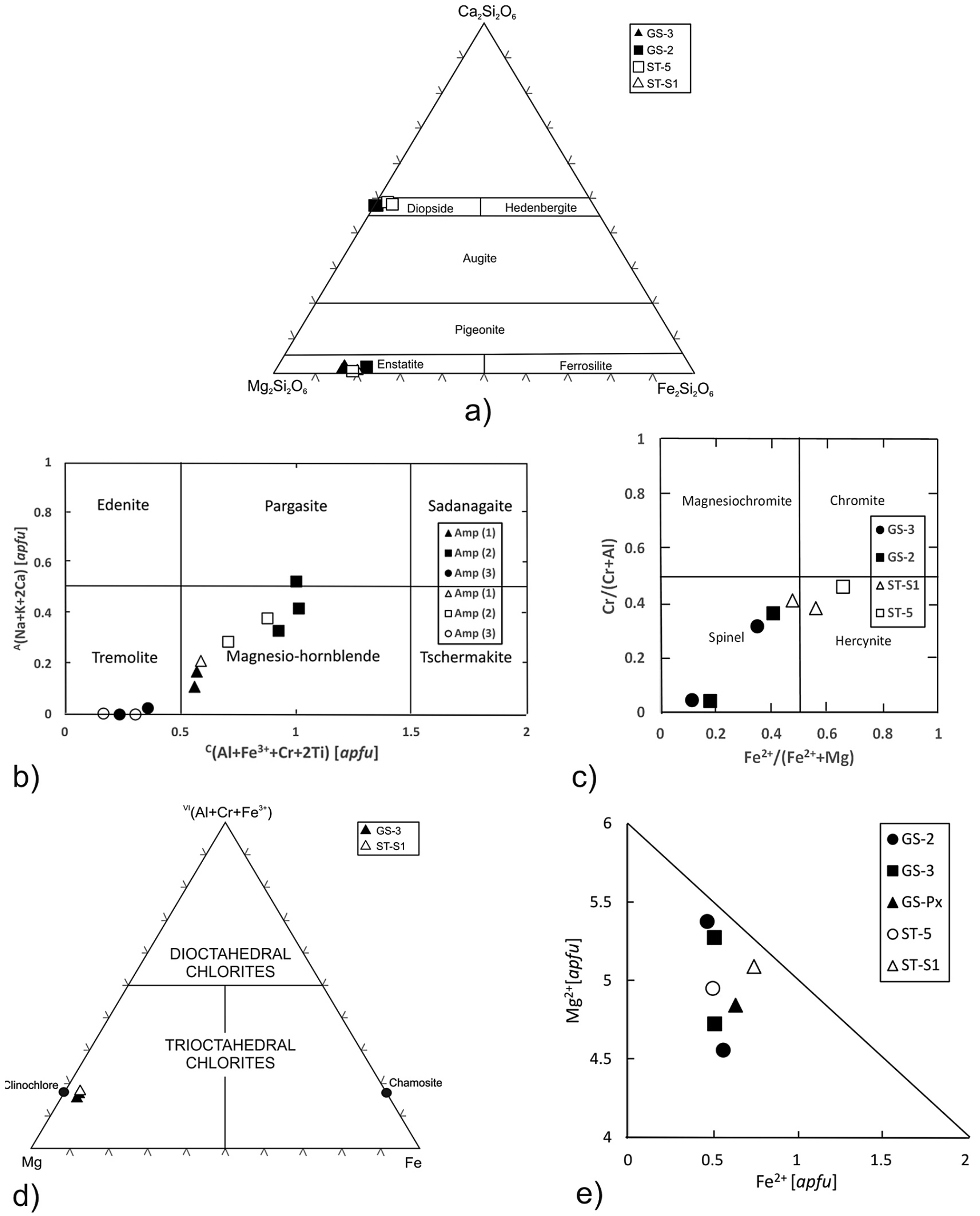

Fig. 5. Classification diagrams **a)** pyroxenes after Morimoto et al. (1988), **b)** amphiboles after Hawthorne et al. (2012), **c)** the spinel group after Lindsley (1991) and **d)** chlorite after Zane and Weiss (1998); with **e)** serpentine group minerals after Bačík (unpublished). Empty symbols: chosen mineral analyses of meta-harzburgites; filled symbols: chosen mineral analyses of meta-pyroxenites.

Obr. 5. Klasifikačné diagramy a) pyroxénov (Morimoto et al., 1988), b) amfibolov (Hawthorne et al., 2012), c) minerálov spinelovej skupiny (Lindsley, 1991) a d) chloritu (Zane a Weiss, 1998); s minerálmi serpentínovej skupiny e) podľa Bačíka (nepublikovaný). Nevyplnené symboly: vybrané analýzy minerálov z meta-harzburgitu; vyplnené symboly: vybrané analýzy minerálov z meta-pyroxenitu.

by Atg or Ctl (Fig. 4c). Low-Al Cpx exsolution lamellae often occur in Opx porphyroblasts and low-Al Opx exsolution lamellae occur in Cpx porphyroblasts. Metamorphic low-Al Opx has enstatitic composition with Mg content between 1.73 and 1.83 *apfu* found from 44 analyses (Fig. 5a; Tab. 4).

Clinopyroxene is Al-poor and occurs as anhedral grains 0.2 to 0.6 mm in metamorphic matrix (Fig. 4c-e). Low-Al Cpx exsolution lamellae are often observable in the core of Mhb (Fig. 4e). Cpx is diopside, containing 0.95 to 1.00 Ca *apfu* found from 43 analyses (Fig. 5a; Tab. 4).

Amphiboles occur as elongated and randomly oriented porphyroblasts with chemical zoning (Fig. 4a–f). Amphibole is composed of magnesio-hornblende core and pargasitic rim, partly replaced by Tr (Figs 4e, 5b; Tab. 5). The inner zone of magnesio-hornblende core often shows Cpx exsolution lamellae and it is rimmed by outer zone of the similar magnesio-hornblende composition but richer in Al, Na, K and Ti. Pargasite occurs also as individual grains in the metamorphic matrix with Cpx and Opx (Fig. 5b; Tab. 5). Tremolite is younger Amp generation occurring in the metamorphic matrix with Cpx, or it ingrows Cpx and Opx porphyroblasts (Fig. 4c,e,f).

Spinel group minerals occur mainly as rounded inclusion in Opx and as anhedral grains of variable size in the metamorphic matrix. According to crystal-chemical formula, it is Spl with Cr from 0.05 to 0.7 *apfu* found from 13 analyses(Figs 4b,f; 5c; Tab. 4). Along with Spl, Mag occurs as opaque mineral.

Chlorite occurs as big flakes, replacing Ol or Opx (Fig. 4e). In classification diagram, it falls into the clinochlore composition (Fig. 5d). It is Mg-rich, containing ca. 4.5 Mg *apfu* (Tab. 6).

Serpentine group minerals Atg/Ctl replace Opx or Ol. They also occur in aggregates with tremolitic amphibole (Figs 4c,d, 5e; Tab. 6).

Tab. 3 Representative mineral analyses of Atg, Ctl and Chl in meta-harzburgite.

Tab. 3 Reprezentačné analýzy Atg, Ctl a Chl v meta-harzburgite.

Sample	ST-5	ST-S1	ST-5	ST-S1	ST-5	ST-S1
Mineral	Atg	Atg	Ctl	Ctl	Chl	Chl
Analyses No.	An 21	An 6	An 19	An 7	An 11	An 18
wt%						
SiO_2	40.09	37.34	41.76	37.95	30.92	30.66
TiO_2	0.00	0.01	0.00	0.00	0.03	0.03
Al_2O^3	0.77	2.38	1.71	0.07	19.50	19.71
Cr_2O_3	0.03	0.20	0.31	0.00	1.05	1.08
FeO	7.48	8.70	6.12	5.15	3.12	3.03
MnO	0.19	0.29	0.22	0.12	0.02	0.05
MgO	35.96	33.30	33.92	39.76	31.71	32.29
NiO	0.38	0.09	0.07	0.27	0.19	0.16
CaO	0.15	0.10	0.09	0.07	0.07	0.00
Na_2O	0.02	0.01	0.00	0.03	0.02	0.01
K_2O	0.03	0.01	0.01	0.02	0.01	0.02
Total	85.10	82.41	84.23	83.44	86.63	87.04
a.p.f.u.						
Si^{4+}	3.949	3.830	4.090	3.794	2.930	2.893
$^{IV}Al^{3+}$	0.051	0.170	0.000	0.206	1.070	1.107
T-sum.	4.000	4.000	4.090	4.000	4.000	4.000
Ti^{4+}	0.000	0.001	0.000	0.000	0.002	0.002
$^{VI}Al^{3+}$	0.089	0.288	0.197	0.009	0.893	0.914
Cr^{3+}	0.003	0.016	0.024	0.000	0.079	0.081
V^{3+}	0.616	0.746	0.502	0.431	0.247	0.239
Fe^{2+}	0.016	0.025	0.018	0.010	0.002	0.004
Mn^{2+}	5.281	5.092	4.952	5.925	4.479	4.543
Mg^{2+}	0.000	0.000	0.000	0.000	0.000	0.000
Zn^{2+}	0.031	0.008	0.006	0.022	0.015	0.013
Ni^{2+}	0.016	0.011	0.009	0.008	0.007	0.000
Ca^{2+}	0.004	0.002	0.000	0.006	0.003	0.001
Na^{+}	0.003	0.001	0.002	0.003	0.001	0.002
K^{+}	6.059	6.188	5.711	6.412	5.727	5.799
M-sum.	6.059	6.188	5.711	6.412	4.942	4.970

5. DISCUSSION

The Austroalpine Sieggraben structural complex shows three deformation-recrystallization stages (D1 to D3) according to Putiš et al. (2000, 2002), Kromel et al. (2011), Hrvanović et al. (2014). The investigated meta-harzburgites and meta-pyroxenites can also be characterized by three metamorphic stages (D1 to D3).

D1 burial stage is interpretable according to typical metamorphic mineral phases of low-Al Opx and Cpx, Fe-rich Ol and sometimes Cr-rich Spl in both principal lithologies. The D1 stage is characteristic by zonal Amp grains with increasing Na and Al from core to rim; the core zones often show low-Al Cpx exsolution lamellae, and all of this indicates a prograde (burial) metamorphic process. The D1 mineral assemblage is consistent with the eclogite facies conditions.

The decomposition of higher-Cr Spl(1) into symplectitic Spl(2, Cr-poor) ingrowing Ol might indicate decompression during the D2 exhumation stage. This assemblage is stable in higher amphibolite- to granulite facies conditions.

Aggregates of Atg/Ctl and Mg-Chl as alteration products of Ol, Opx and Spl, and replacement of Spl by Mag, indicate continuing decompression and cooling, therefore interpretable as inferred the D3 exhumation stage. Tremolite as the darkest external part of zonal Amp grains along with Srp, Mg-Chl and Mag indicates a retrograde metamorphic process in amphibolite- to higher greenschist facies conditions.

The D1 to D3 evolution stages most likely occurred in Cretaceous, as reported from other parts of the HP-bearing Austroalpine basement fragments (e.g., Thöni and Jagoutz 1993; Thöni 1999; Thöni et al. 2008).

6. CONCLUSIONS

Investigated ultramafic rocks are composed of typical metamorphic mineral phases: Fe-rich Ol, Al-poor Opx, Al-poor Cpx, zonal Amp (Mhb, Prg to Tr), Cr-poor and Cr-rich

Tab. 4 Representative mineral analyses of Ol, Opx, Cpx and Spl in meta-pyroxenite.

Tab. 4 Reprezentačné analýzy Ol, Opx, Cpx a Spl v meta-pyroxenite.

Sample	GS-2c	GS-2c	GS-2a	GS-2a	GS-2a	GS-2a	GS-3-1	GS-2c	GS-3-3a	GS-2c
Mineral	Ol	Ol	Opx	Opx	Cpx	Cpx	Spl	Spl	Spl	Spl
Analyses No.	An 17	An 19	An 6	An 7	An 8	An 9	An 9	An 18	An 1	An 29
wt %										
SiO_2	41.08	41.17	56.85	56.43	54.33	54.19	0.05	0.06	2.44	0.07
TiO_2	0.00	0.00	0.03	0.03	0.02	0.01	0.09	0.00	0.02	0.00
Al_2O_3	0.00	0.00	1.18	1.90	0.73	0.45	36.32	62.04	59.29	36.02
V_2O_3	0.00	0.00	0.00	0.00	0.00	0.00	0.06	0.00	0.05	0.05
FeO	7.75	7.57	5.48	5.40	1.40	1.16	22.61	10.60	11.41	19.19
MnO	0.23	0.19	0.21	0.15	0.04	0.09	0.28	0.11	0.15	0.54
MgO	51.20	51.06	35.82	34.85	18.00	18.12	15.00	21.31	22.79	13.50
CaO	0.03	0.02	0.13	0.27	24.97	25.22	0.08	0.02	0.22	0.12
Na_2O	0.00	0.00	0.00	0.00	0.08	0.06	0.00	0.00	0.00	0.00
K_2O	0.00	0.00	0.01	0.00	0.00	0.00	0.00	0.00	0.00	0.00
Cr_2O_3	0.04	0.01	0.18	0.18	0.21	0.21	25.05	4.11	4.16	30.72
NiO	0.43	0.52	0.16	0.16	0.12	0.04	0.28	0.45	0.27	0.06
Total	100,76	100,53	100,06	99,36	99,90	99,55	99,82	98,70	100,80	100,29
a.p.f.u.										
Si^{4+}	0.990	0.994	1.948	1.951	1.970	1.968	0.000	0.00	0.00	0.00
Ti^{4+}	0.000	0.000	0.001	0.001	0.001	0.000	0.002	0.000	0.000	0.000
Al^{3+}	0.000	0.000	0.048	0.077	0.030	0.019	1.229	1.867	1.779	1.230
Cr^{3+}	0.001	0.000	0.005	0.005	0.006	0.006	0.569	0.083	0.085	0.704
Fe^{3+}	0.000	0.000	0.049	0.015	0.028	0.044	0.201	0.050	0.135	0.067
Fe^{2+}	0.156	0.153	0.108	0.141	0.015	0.000	0.342	0.177	0.112	0.398
Mg^{2+}	1.839	1.838	1.830	1.796	0.965	0.981	0.642	0.811	0.880	0.583
Mn^{2+}	0.005	0.004	0.006	0.004	0.001	0.003	0.007	0.002	0.003	0.013
Ca^{2+}	0.001	0.000	0.005	0.010	0.970	0.981	0.002	0.000	0.000	0.004
Ni^{2+}	0.008	0.010	0.000	0.000	0.000	0.000	0.007	0.009	0.005	0.001
Total	3,000	3,000	4,000	3,999	3,985	4,003	3,000	3,000	3,000	3,000
Fo	92.179	92.328								
Wo					48.165	48.661				
En					51.071	51.816				
Fs					0.764	0.000				
2Ti/(2Ti+Al+Cr)							0.002	0.000	0.000	0.000
$2Fe^3$+/($2Fe^{3+}$+Al+Cr)							0.182	0.049	0.127	0.064
Fe^2+/(Fe^{2+}+Mg)							0.348	0.179	0.113	0.406
Cr/(Cr+Al)							0.316	0.043	0.046	0.364

minerals of the spinel group, Atg/Ctl mineral of the serpentine group and chlorite. Modal estimates speak for original harzburgite crosscut by pyroxenite dikes.

Meta-harzburgites are composed of mainly metamorphic olivine-orthopyroxene aggregates inherited from a harzburgitic protolith. Meta-harzburgites show a distinct metamorphic recrystallization of inferred original harzburgite magmatic phases (Ol, Opx, Spl ±Cpx) transposed to the D1 eclogite-facies Fe-Ol, low-Al Opx and Cpx, Mg-Hbl to Prg, Cr-Spl (D1) during burial in a subduction channel.

Meta-pyroxenite contains mainly metamorphic Cpx and Opx indicating a pyroxenite protolith. Porphyroblasts of low-Al Opx, low-Al Cpx, Fe rich Ol and Cr-Spl suggest eclogite-facies metamorphic conditions characteristics for the D1 metamorphic stage.

The D2 exhumation stage is recognized by the Ol-Spl (after Cr-Spl) symplectites.

The D3 metamorphic stage is determined by the amphibolite- to greenschist facies mineral metamorphic association composed of the serpentine-group minerals (Ctl/Atg), clinochlore, tremolite and magnetite.

Tab. 5 Representative chemical composition of Amp in meta-pyroxenite.
Tab. 5 Reprezentačné analýzy Amp v meta-pyroxenite.

Sample name	GS-3-1	GS-3-1	GS-3-1	GS-3-1	GS-3-1	GS-3-1
Mineral	Mhb	Mhb	Prg	Mhb	Tr	Tr
Analyses No.	An 16	An 44	An 19	An 36	An 20	An 27
wt%						
SiO_2	52.36	51.97	44.84	47.26	56.41	54.87
TiO_2	0.21	0.20	0.40	0.40	0.12	0.23
Al_2O_3	6.97	6.18	11.05	11.60	2.96	3.85
Cr_2O_3	0.21	0.30	0.53	0.66	0.07	0.17
FeO	3.50	3.35	4.85	4.92	2.49	3.06
MnO	0.05	0.04	0.05	0.04	0.02	0.04
MgO	20.54	20.75	18.50	18.45	22.31	21.56
NiO	0.20	0.16	0.13	0.18	0.15	0.14
CaO	13.25	12.90	12.88	12.93	13.42	13.23
Na_2O	0.63	0.62	1.31	1.02	0.20	0.23
K_2O	0.25	0.06	0.95	0.85	0.05	0.06
Cl	0.06	0.04	0.12	0.08	0.02	0.03
Total	98.23	96.58	95.61	98.38	98.20	97.45
a.p.f.u.						
Si^{4+}	7.215	7.260	6.457	6.600	7.700	7.569
Al^{3+}T	0.785	0.740	1.543	1.400	0.300	0.431
T-sum.	8.000	8.000	8.000	8.000	8.000	8.000
Ti^{4+}	0.022	0.021	0.044	0.042	0.012	0.024
Al^{3+}Z	0.347	0.277	0.332	0.510	0.176	0.195
Cr^{3}+	0.023	0.034	0.061	0.073	0.007	0.019
V^{3+}	0.000	0.000	0.000	0.000	0.000	0.000
Mg^{2+}	4.221	4.321	3.971	3.841	4.540	4.434
Mn^{2+}	0.006	0.004	0.006	0.004	0.002	0.004
Fe^{3+}	0.158	0.208	0.522	0.305	0.030	0.098
Fe^{2+}	0.245	0.184	0.062	0.269	0.254	0.255
Zn^{2+}	0.000	0.000	0.000	0.000	0.000	0.000
Ni^{2+}	0.023	0.019	0.016	0.021	0.017	0.016
C-sum.	5.043	5.069	5.013	5.066	5.038	5.044
Ca^{2+}	1.957	1.931	1.987	1.934	1.962	1.956
Na^{+}	0.043	0.069	0.013	0.066	0.038	0.044
B-sum.	2.000	2.000	2.000	2.000	2.000	2.000
Na^{+}	0.126	0.099	0.354	0.210	0.016	0.017
K^{+}	0.045	0.011	0.174	0.151	0.009	0.010
A-sum.	0.170	0.110	0.528	0.361	0.025	0.027
Cl^{-}	0.014	0.010	0.029	0.020	0.005	0.006
OH^{-}	1.986	1.990	1.971	1.980	1.995	1.994

Tab. 6 Representative mineral analyses of Atg, Ctl and Chl in meta-pyroxenite.
Tab. 6 Reprezentačné analýzy Atg, Ctl and Chl v meta-pyroxenite.

Sample	GS-3-1	GS-2a	GS-2c	GS-2c	GS-3-1	GS-3-2
Mineral	Atg	Atg	Ctl	Ctl	Chl	Chl
Analyses No.	An 25	An 12	An 9	An 33	An 26	An 2
wt %						
SiO_2	39.48	45.45	48.10	40.58	30.29	30.72
TiO_2	0.02	0.02	0.00	0.00	0.06	0.05
Al_2O_3	2.60	1.52	0.05	1.45	19.45	20.24
Cr_2O_3	0.16	0.21	0.00	0.00	0.70	0.30
FeO	8.43	7.13	6.09	5.79	3.62	3.27
MnO	0.11	0.14	0.20	0.22	0.03	0.02
MgO	34.35	32.27	31.05	37.28	31.96	31.58
NiO	0.12	0.12	0.05	0.19	0.27	0.21
CaO	0.08	0.17	0.16	0.18	0.00	0.02
Na_2O	0.02	0.61	0.01	0.02	0.02	0.00
K_2O	0.00	0.43	0.04	0.01	0.00	0.08
Total	85.36	88.08	85.76	85.71	86.40	86.49
a.p.f.u.						
Si^{4+}	3.884	4.264	4.547	3.926	2.888	2.911
$^{IV}Al^{3+}$	0.116	0.000	0.000	0.074	1.112	1.089
T-sum.	4.000	4.264	4.547	4.000	4.000	4.000
Ti^{4+}	0.001	0.002	0.000	0.000	0.004	0.003
$^{VI}Al^{3+}$	0.301	0.169	0.005	0.165	0.926	0.828
Cr^{3+}	0.012	0.016	0.000	0.000	0.053	0.022
V^{3+}	0.694	0.559	0.481	0.468	0.288	0.259
Fe^{2+}	0.010	0.011	0.016	0.018	0.003	0.001
Mn^{2+}	5.037	4.514	4.376	5.377	4.543	4.462
Mg^{2+}	0.000	0.000	0.000	0.000	0.000	0.000
Zn^{2+}	0.010	0.009	0.004	0.015	0.022	0.017
Ni^{2+}	0.008	0.017	0.017	0.018	0.000	0.002
Ca^{2+}	0.003	0.111	0.002	0.004	0.004	0.000
Na^{+}	0.000	0.052	0.005	0.001	0.000	0.009
K^{+}	6.077	5.460	4.907	6.067	5.843	5.604
M-sum.	6.077		4.907	6.067	4.990	4.949

Meta-harzburgites and meta-pyroxenites exposed between the Steinbach and Gschorrholz villages are the mantle fragments emplaced in subducted lower continental crust during the Cretaceous subduction-collision event.

Acknowledgements: This investigation was supported by the APVV-0081-10, VEGA-1/0255/11 and VEGA-1/0079/15 scientific grants (M.P.). Suggestions of F. Koller (Vienna University), R. Schuster (Geological Survey of Austria in Vienna) and M. Kováčik (State Geological Institute of D. Stur in Bratislava) are greatly acknowledged. We also thank R. Marshall for reviewing the English content.

7. REFERENCES

Dallmeyer R. D., Neubauer F., Handler R., Fritz H., Müller W., Pana D. & Putiš M., 1996: Tectonothermal evolution of the internal Alps and Carpathians: evidence from $^{40}Ar/^{39}Ar$ mineral and whole-rock data. *Eclogae Geologicae Helvetiae*, 89, 1, 203–227.

Dallmeyer R.D., Handler F., Neubauer F. & Fritz H., 1998: Sequence of thrusting within a thick-skinned tectonic wedge: evidence from $^{40}Ar/^{39}Ar$ and Rb–Sr ages from the Austroalpine nappe complex of the Eastern Alps. *Journal of Geology*, 106, 71–86.

Frank W., Kralik M., Scharbert S. & Thöni M., 1987: Geochronological data from the Eastern Alps. *In*: Flügel H. W., Faupl P. (Eds.): Geodynamics of the Eastern Alps. F. Deuticke, Vienna, pp. 272–281.

Frisch W. & Neubauer F., 1989: Pre-Alpine terranes and tectonic zoning in the Eastern Alps. *In:* Dallmayer R.D. (Ed.): Terranes in the Circum-Atlantic Paleozoic orogens. Special Paper, Geological Society of America, 230, 91–100.

Froitzheim N., Schmid S. M. & Frey M., 1996: Mesozoic paleogeography and the timing of eclogite-facies metamorphism in the Alps: A working hypothesis. *Eclogae Geologicae Helvetiae*, 89, 81–110.

Hawthorne C. F., Oberti R., Harlow G., Maresch V. W., Schumaher C. J. & Welch M., 2012: Nomenclature of the amphibole supergroup. *American Mineralogist, 97, 2031–2048.*

Hrvanović S., Putiš M. & Bačík P., 2014: Petrography and mineral chemistry of metaultramafics in the Austroalpine Sieggraben structural complex at Sieggraben and Schwarzenbach, Austria. *Bulletin mineralogicko-petrologického odděleního muzea v Praze,* 22, 105–114.

Korikovsky S. P., Putiš M., Kotov A. B., Salnikova E. B. & Kovach V. P., 1998: High-pressure metamorphism of the phengite gneisses of the Lower Austroalpine nappe complex in the Eastern Alps: mineral equilibria, P-T parameters, and age. *Petrology*, 6, 603–619.

Kromel J., Putiš M. & Bačík P., 2011: The Middle Austro-Alpine Sieggraben structural complex - new data on geothermobarometry. *Acta Geologica Slovaca* 3, 1–12.

Kümel F., 1935: Die Sieggrabener Deckscholle im Rosaliengebirge (Nieder Österreich–Burgenland). *Tschermaks Mineralogische und Petrographische Mitteilugen*, 47, 141–184.

Lindsley D. H., 1991: Oxide minerals: petrologic and magnetic significance. *Reviews in Mineralogy,* 25, 509 p.

Morimoto N., Fabries J., Ferguson A. K., Ginzburg I. V., Ross M., Seifert F. A. & Zussman J., 1988: Nomenclature of pyroxenes. *American Mineralogist,* 73, pp. 1123–1133.

Neubauer F., 1994: Kontinentkollision in den Ostalpen. *Geowissenschaften,* 12, 136–140.

Neubauer F. & Frich W., 1993: The Austro-Alpine metamorphic basement east of the Tauern Window. *In:* von Raumer J. F. & Neubauer F. (Eds.): The Pre-Mesozoic geology of the Apls. Springer Verlag, Heidelberg, pp. 515–535.

Neubauer F., Müller W., Peindl P., Mozschewitz E., Wallbrecher E. & Thöni M., 1992: Evolution of lower Austroalpine units along the eastern margins of the Alps: a review. *In*: Neubauer F. (Ed.): ALCAPA-Field Guide. University Graz, pp. 97–114.

Putiš M., Korikovsky S. P., Pushkarev Y. D. & Zakariadze G. S., 1994: Geology, tectonics, petrology, geochemistry and isotope dating of the Sieggraben (Grobgneis and Wechsel) Unit in the Eastern Alps. Manuscripts, Geological Survey of Austria, Vienna, 154 p.

Putiš M., Korikovsky S. P. & Pushkarev Y. D., 2000: Petrotectonics of an Austroalpine eclogite-bearing complex (Sieggraben, Eastern Alps) and U-Pb dating of exhumation. *Jahrbuch der Geologischen Bundesanstalt*, 142, 73–93.

Putiš M., Korikovsky S. P., Wallbrecher E., Unzog W., Olesen N. O. & Fritz H., 2002: Evolution of an eclogitized continental fragment in the Eastern Alps (Sieggraben, Austria). *Journal of Structural Geology,* 24, 339–357.

Schmid M., Fügenschuh B., Kissling E. & Schuster R., 2004: Tectonic map and overall architecture of the Alpine orogen. *Eclogae Geologicae Helvetiae*, 97, 93–117.

Thöni M., 1999: A review of geochronological data from the Eastern Alps. *Schweizerische Mineralogische und Petrographische Mitteilungen*, 79, 209–230.

Thöni M. & Jagoutz E., 1993: Isotopic constraints for eo-Alpine high-P metamorphism in the Austroalpine nappes of the Eastern Alps: Its Bearing on Alpine orogenesis. *Schweizerische Mineralogische und Petrographische Mitteilungen*, 73, 177–189.

Thöni M., Miller C., Blichert-Toft J., Whitehouse M. J., Konzett J. & Zanetti, A., 2008: Timing of high-pressure metamorphism and exhumation of the eclogite type-locality (Kupplerbrunn-Prickler Halt, Saualpe, south-eastern Austria): constraints from correlations of the Sm-Nd, Lu-Hf, U-Pb and Rb-Sr isotopic systems. *Journal of Metamorphic Geology*, 26, 561–581.

Tollmann A., 1977: Geologie von Östtereich. Band I: Die Zentralalpen. Deuticke, Vienna.

Tollmann A., 1980: Geology and tectonics of the Eastern Alps (Middle Sector). *Abhandlungen der Geologischen Bundesanstalt, Wien*, 34, 197–255.

Whitney D. L. & Evans B. W., 2010: Abbreviations for names of rock-forming minerals. *American Mineralogist*, 95, 185–187.

Zane A. & Weiss, Z., 1998: A procedure for classifying rock-forming chlorites based on microprobe data. *Rendiconti Lincei,* 9, 51–56.